ISSN 1070-4280, Russian Journal of Organic Chemistry, 2023, Vol. 59, No. 9, pp. 1598–1609. © Pleiades Publishing, Ltd., 2023.

Microwave-Assisted Synthesis of β-Cyanoketones under Bucherer–Bergs Conditions and Their Antimicrobial Evaluation and In Silico Studies

M. A. Leyva-Acuña[a], F. Delgado-Vargas[a,b], G. Lopez-Angulo[a], Y. P. Ahumada-Santos[c], I. A. Rivero[d], S. Durán-Pérez[c], and J. Montes-Avila[a,b,*]

[a] *Programa de Posgrado Integral en Biotecnología, Facultad de Ciencias Químico-Biológicas, Universidad Autónoma de Sinaloa, Culiacán, Sinaloa, 80010 Mexico*

[b] *Programa de Posgrado en Ciencias Biomédicas, Facultad de Ciencias Químico-Biológicas, Universidad Autónoma de Sinaloa, Culiacán, Sinaloa, 80010 Mexico*

[c] *Facultad de Ciencias Químico-Biológicas, Universidad Autónoma de Sinaloa, Culiacán, Sinaloa, 80010 Mexico*

[d] *Instituto Nacional de México, Centro de Graduados e Investigación en Química, Tijuana, Baja California, 22000 Mexico*

**e-mail: jmontes@uas.edu.mx*

Received October 22, 2022; revised November 26, 2022; accepted November 26, 2022

Abstract—The microwave-assisted synthesis of β-cyanoketones from chalcones under Bucherer–Bergs reaction conditions was described. The structure of the synthesized compounds was elucidated by FTIR-ATR, ^{1}H and ^{13}C NMR, MS/CI, and elemental analyses. All compounds were evaluated for their in vitro antibacterial against three Gram-positive and four Gram-negative bacterial strains. Moreover, their in vitro toxicity was evaluated by the *Artemia salina* assay, and the most active antibacterial agents were analyzed in silico.

Keywords: β-cyanoketones; Bucherer-Bergs; microwave; antimicrobial activity; docking

DOI: 10.1134/S107042802309018X

INTRODUCTION

Bacterial infections are a public health concern worldwide associated with drug resistance development. Such antimicrobial resistance is currently responsible for more than 700000 deaths annually, estimated to reach more than 10 million deaths/year by 2050 with a cost of $100 million [1]. Therefore, the development of new antibacterial agents is in continuous demand.

Researchers in medicinal chemistry have isolated from natural sources and synthesized nitrile-containing compounds to treat different diseases; examples are letrozole (anticancer drug) and etravirine (anti-HIV drug) [2]. Accordingly, incorporating a cyano group (C≡N) in biologically active compounds is a promising rational drug design strategy to improve their characteristics, including enhanced binding affinity to the target, better pharmacokinetics, and reduced drug resistance [3]. Thus, nitrile chemistry is attractive for designing novel antimicrobial agents.

β-Cyanoketones are valuable synthons in organic synthesis; they are commonly obtained by conjugate hydrocyanation of α,β-unsaturated ketones (Michael acceptors) [4]. The cyano group in β-cyanoketones is a building block for synthesizing other biologically active compounds, such as amines [5], heterocycles [6], esters [7], and carboxylic acids [8]. Furthermore, β-cyano adducts are intermediate products in the synthesis of antidepressant agents and selective agonists of GABA receptors such as γ-aminobutyric and γ-lactam acids [9–11]. Therefore, many methods have been reported for the synthesis of β-cyano carbonyl compounds using different nitrile reagents and catalysts, such as TEACN/scandium(III) trifluoromethanesulfonate [12], malononitrile/KF–Al_2O_3 [13], ethyl cyano-

acetate with KOH as a base [14], ketone cyanohydrins/$NiCl_2$ (complexes) [15], nucleophilic cyanide attack on cyclic vinyl carbonates [16], and TMSCN under microwave irradiation [17] or catalysts like CsF [18] and Amberlite® IRA 900F [19]. However, these processes usually employ expensive or non-commercial reagents and long reaction times (3–24 h), showing low regioselectivity, and sometimes HCN is produced. Hence, the development of better procedures for the synthesis of β-cyanoketones remains a challenge. Although organic nitriles are essential components in more than 30 currently prescribed drugs [20], biological activities of β-cyanoketones obtained from chalcones have not been reported up to date.

Previously, our research group synthesized and characterized chalcones with antiparasitic, and antioxidant activities [21, 22]. It has also been reported that the antibacterial activities of chalcones are associated with the inhibition of dihydrofolate reductase (DHFR) [23–25]. The same mechanism is used by trimethoprim [26]. In the present work, β-cyanoketones **2a**–**2j** were synthesized from chalcones **1a–1j** via the Bucherer–Bergs reaction under microwave irradiation. The obtained β-cyanoketones were evaluated against human pathogenic bacteria (Gram-positive and Gram-negative), and their toxicity to *Artemia salina* was determined. In addition, in silico analysis of β-cyanoketones was performed to obtain their ADMET (absorption, distribution, metabolism, excretion, toxicity) properties and interaction with dihydrofolate reductase (DHFR) by molecular docking. The in vitro and in silico results showed for the first time the antimicrobial potential of β-cyanoketones.

RESULTS AND DISCUSSION

Eleven racemic β-cyanoketones **2a**–**2l** were smoothly synthesized through the Bucherer–Bergs reaction of previously prepared chalcones **1a**–**1l** [21, 22] with KCN and $(NH_4)_2CO_3$ in MeOH/H_2O] [37, 38] under microwave irradiation (Scheme 1). The best reaction conditions were temperature of 100°C and irradiation time of 20 min. At shorter irradiation times, either no products were formed or their yields were poor (around 10%), whereas longer irradiation times caused polymerization. The Bucherer–Bergs reaction commonly utilizes 50% aqueous alcohol where both KCN and $(NH_4)_2CO_3$ are readily soluble [26]. The reactions were also carried out under conventional heating (at reflux temperature), but they did not proceed up to 24 h, and the reaction mixtures contained unchanged chalcone (TLC). Li et al. [39] found that strong bases such as KOH or NaOH are essential in the hydrocyanation of chalcones that proceeds through Michael 1,4-addition [39]. In this sense, $(NH_4)_2CO_3$ is indispensable for forming hydantoins in the Bucherer–

Scheme 1.

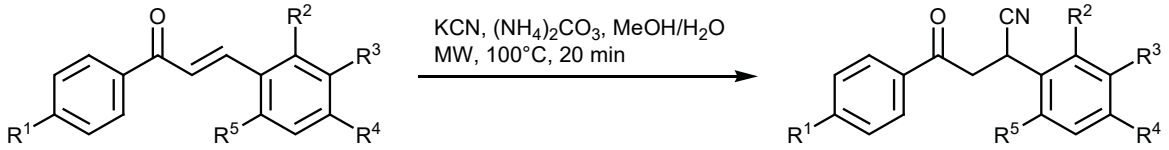

1a–1l **2a–2l**

Compd. no.	R^1	R^2	R^3	R^4	R^5	Yield, %	mp, °C
2a	H	H	H	Me	H	82.5	132–134
2b	Me	H	H	Me	H	81.0	108–109
2c	Cl	Me	H	Me	Me	80.4	115–117
2d	OMe	H	H	H	H	88.0	103–105
2e	H	H	H	OMe	H	92.0	105–107
2f	OMe	H	H	Me	H	83.0	86–88
2g	Me	H	H	OMe	H	91.0	85–87
2h	OMe	H	H	OMe	H	87.0	100–102
2i	OMe	H	H	Cl	H	80.2	88–90
2j	H	H	H	4*H*-Pyran-3-yloxy	H	50.4	96–99
2k	H	H	H	H	OH	72.0	146–149
2l	H	H	OH	OH	H	74.0	105–108

Bergs reaction. The carbonate could stabilize the enolate ion to make the addition of cyanide ion irreversible, leading to the selective synthesis of β-cyanoketones under less aggressive conditions; no HCN was detected during the reaction despite using KCN as a cyanide source.

The highest yields of β-cyanoketones (80–92%) were obtained when an electron-donating group (Me or OMe) was present at the *para* position of ring B, and lower yields (50–74%) were obtained with OH or pyran groups (Scheme 1). The poor performance of OH-containing compounds may be due to losses during the extraction and purification processes. Compared with other hydrocyanation methods, the proposed method uses cheaper reagents and requires shorter reaction times. Furthermore, the yields were similar to those reported by other researchers. For example, the use of ethyl cyanoacetate as a source of cyanide and KOH for 8 h provided β-cyanoketones in a yield of 55–93% [14]. The direct conversion of cyanohydrins and aldehydes or ketones to β-cyanoketones by nickel-catalyzed cyano-borrowing reaction at 100°C for 18 h yielded 56–90% [15]. It is highlighted that reports on the synthesis of β-cyanoketones are scarce.

The spectroscopic data (FTIR-ATR, ^{1}H and ^{13}C NMR, GC/MS) and elemental analyses of purified β-cyanoketones **2a**–**2l** agreed with the expected structures. Compounds **2c**, **2h**, **2i**, **2j**, **2k**, and **2l** were not reported previously. For example, the IR spectrum of **2i** showed absorption bands at 3006 and 2918 cm^{-1} for stretching vibrations of aromatic and aliphatic C–H bonds, a band at 2243 cm^{-1} due to C≡N stretchings, a strong band at 1670 cm^{-1} for C=O stretching vibrations, bands at 1249 and 1025 cm^{-1} for asymmetric and symmetric C–O–C stretchings, and a band at 759 cm^{-1} due to C–Cl stretching. The ^{1}H NMR spectrum of **2i** showed signals in the region of δ 7.90–6.93 ppm for the eight aromatic hydrogens, a doublet of doublets at δ 4.56 ppm with ^{3}J = 6.0 and 8.0 Hz for the proton attached to the asymmetric carbon atom, a singlet at δ 3.87 ppm for the methoxy group, and two doublets of doublets at δ 3.67 and 3.44 ppm for the magnetically nonequivalent α-methylene hydrogens with geminal (^{2}J = 18.0 Hz) and vicinal (^{3}J = 8.0 Hz) couplings. The ^{13}C NMR spectrum of **2i** showed 13 expected carbon signals attributable to 17 carbons, comprising six quaternary carbons, nine CH, one CH_2, and one CH_3, in agreement with the formula $C_{17}H_{14}ClNO_2$. In particular, the signal at δ_C 192.7 ppm was assigned to the ketone carbonyl carbon, eight signals between δ_C 164.1 and 114.0 ppm corresponded to aromatic carbons, the signal at δ_C 120.4 ppm belonged to the cyano group, and the signals at δ_C 43.8 and 31.4 ppm were assigned to the CH_2 and chiral CH groups. The chemical ionization mass spectrum of **2i** displayed a quasi-molecular ion peak at *m*/*z* 300 $[M + H]^+$. Additionally, the electron impact mass spectrum of **2i** contained the molecular ion peak at *m*/*z* 299 $[M]^+$ with moderate intensity, and the base peak was that observed at *m*/*z* 135, which was attributed to C_α–C(O) bond cleavage.

Our research team previously reported that chalcones **1a**–**1j** used as precursors in the synthesis of the β-cyanoketones **2a**–**2j** were inactive against the bacterial strains tested [21]. However, most β-cyanoketones **2a**–**2j** were bacteriostatic at 200 μg/mL on both Gram-positive and Gram-negative bacteria (Table 1). In this regard, five β-cyanoketones (**2a**, **2b**, **2f**, **2g**, **2i**) showed the highest activity against *E. coli* (ATCC 25922) (MIC = 12.5–50 μg/mL; MBC = 50–100 μg/mL), **2a**, **2b**, and **2f** being the most active (MIC = 12.5–25 μg/mL; MBC = 50 μg/mL). Likewise, only compound **2g** showed bactericidal activity against *S. typhi* at (MIC = MBC = 100 μg/mL) and *P. aeruginosa* (ATCC 27853) (MIC = 50 μg/mL and MBC = 200 μg/mL). In contrast, *E. faecalis* (ATCC 29212) was the least sensitive Gram-positive strain, and only **2b** was active against it (MIC = 100 μg/mL). The structure–activity analysis showed several patterns. β-Cyanoketone **2b** (R^1 = R^4 = Me) exhibited the highest activity against *E. coli* (ATCC 25922) (MIC = 12.5 μg/mL; MBC = 50 μg/mL). Compounds **2a** and **2f** (R^1 = H, OMe; R^4 = Me) also showed good activities (MIC = 25 μg/mL; MBC = 50–100 μg/mL). On the other hand, the combination of an electron-withdrawing group (Cl) as R^1 and electron-donating groups as R^2, R^4, and R^5 (Me), as well as protection with a pyran group, suppressed the activity of **2c** and **2j**; these substitutions could reduce the molecular polarity and solubility in the medium. Similarly, the incorporation of only strongly activating groups such as OMe and OH (**2d**, **2e**, **2h**, **2k**, **2l**) decreased the activity against most Gram-positive and Gram-negative bacteria. However, the combination of OMe group with Me or Cl (**2g**, **2i**) increased the activity against the Gram-negative bacteria *E. coli* (ATCC 25922), *S. Typhi*, and *P. aeruginosa* (ATCC 27853). In contrast, a slightly increased activity for **2g** was observed against the Gram-positive bacteria *S. aureus* ATCC 25923 and ATCC 29213. A higher susceptibility of Gram-negative bacteria to most β-cyanoketones was demonstrated in comparison to Gram-positive bacteria. A similar anti-

Table 1. Minimum inhibitory concentrations (MIC, μg/mL) and minimal bactericidal concentration (MBC, μg/mL) of β-cyanoketones **2a**–**2l**[a]

Compound no.	Gram-positive						Gram-negative							
	S. aureus 29213		*S. aureus* 25923		*E. faecalis* 29212		*E. coli* 25922		*S.* Typhi		*S. dysenteriae*		*P. aeruginosa* 27853	
	MIC	MBC	MIC	MBC	MIC	MBC	MIC	MBC	MIC	MBC	MIC	MBC	MIC	MBC
2a	200	–	200	–	–	–	25	50	200	–	200	–	200	–
2b	200	–	200	–	200	–	12.5	25	200	–	200	–	200	–
2c	–	–	–	–	–	–	–	–	–	–	–	–	–	–
2d	–	–	–	–	–	–	–	–	–	–	200	–	–	–
2e	–	–	–	–	–	–	–	–	–	–	200	–	–	–
2f	200	–	200	–	–	–	25	50	200	–	200	–	200	–
2g	200	–	200	–	–	–	50	50	100	100	200	–	50	200
2h	–	–	–	–	–	–	–	–	–	–	200	–	–	–
2i	–	–	200	–	–	–	50	100	200	–	200	–	50	–
2j	–	–	–	–	–	–	–	–	–	–	–	–	–	–
2k	–	–	–	–	–	–	–	–	–	–	200	–	–	–
2l	–	–	–	–	–	–	–	–	–	–	200	–	–	–
Gentamicin	0.5	2	0.5	2	4	4	1	1	1	1	1	1	1	4

[a] "–" stands for no activity.

bacterial effect against Gram-negative bacteria, especially on *E. coli*, was reported for nitrile compounds [2]. Bhat et al. [40] recently reported that the introduction of cyano groups into heterocycles (e.g., pyrimidines) increases the ability to penetrate the bacterial cell wall, and the compounds become more active. Furthermore, this antibacterial potential was attributed to the ability of bacteria to hydrolyze nitrile groups to amide to produce an *N*,*O*-bidentate site as a crucial template [41]. Nevertheless, none of the tested β-cyanoketones were more active than the reference drug Gentamicin (0.5–4 μg/mL) [42].

β-Cyanoketones **2a**, **2b**, **2d**–**2i**, **2k**, and **2l** with antibacterial activity were not toxic against *Artemia salina* (% mortality = 0–10%) and obeyed Lipinski's rule of five [43]. Thus, these compounds are potential scaffolds for developing new compounds with improved biological activities.

In drug development, the ideal molecules must show high biological activity and low toxicity. In this regard, in silico analysis provides supporting information for drug development. The analysis with the SwissADME software showed that all β-cyanoketones **2a**–**2l** satisfy Lipinski's rule of five and the bioavailability requirements (Table 2). The numbers of H-bond acceptors were two for compounds **2a**–**2c**, three for **2d**–**2g** and **2i**–**2k**, and four for **2h** and **2l**. On the other hand, all β-cyanoketones showed zero H-donor but **2k** (one H-bond donor) and **2l** (two H-bond donors). These centers helped in H-bond formation, enhancing water solubility. Additionally, the rotatable bonds amounted to four for **2a**, **2c**, **2k**, and **2l**, five for **2d**–**2g** and **2i**, and six for **2b**, **2h**, and **2j**. More rotatable bonds in molecules contribute to their better adaptability and flexibility and hence favor interactions with the target molecule. The log*P* values of the synthesized β-cyanoketones were in the range 2.22–4.53, indicating optimal lipophilicity to penetrate cell membranes and increase bioavailability. Log*P* values lower than –0.5 are associated with poor dissolution in lipids and cell membrane penetration. Likewise, TPSA and MW of molecules affect the transportation through the biological membranes, and desirable values were lower than 500 g/mol MW and 140 Å^2 TPSA. The β-cyanoketones had a positive bioactivity score (*F*), suggesting good bioavailability and results in clinical trials [38]. Moreover, the predicted gastrointestinal (GI) absorption and blood–brain barrier (BBB) permeation were high for all the β-cyanoketones but **2l**.

Table 2. In silico parameters of β-cyanoketones **2a**–**2l**[a]

Compd. no.	MW	NHA	NHD	NRB	TPSA, Å^2	Log*P* (*c*Log*P*)	*F*	Water solubility	GI	BBB	Pgp	Ro5 violations
2a	249.31	2	0	4	40.86	3.40	0.55	Moderate	High	Yes	No	0
2b	295.33	2	0	6	40.86	3.75	0.55	Poor	High	Yes	No	0
2c	311.81	2	0	4	40.86	4.53	0.55	Poor	High	Yes	No	0
2d	265.31	3	0	5	50.09	3.05	0.55	Moderate	High	Yes	No	0
2e	265.31	3	0	5	50.09	3.05	0.55	Moderate	High	Yes	No	0
2f	279.33	3	0	5	50.09	3.38	0.55	Moderate	High	Yes	No	0
2g	279.33	3	0	5	50.09	3.39	0.55	Moderate	High	Yes	No	0
2h	295.33	4	0	6	59.32	3.04	0.55	Moderate	High	Yes	No	0
2i	299.75	3	0	5	50.09	3.59	0.55	Poor	High	Yes	No	0
2j	329.39	3	0	6	50.09	3.89	0.55	Poor	High	Yes	No	0
2k	251.28	3	1	4	61.09	2.64	0.55	Moderate	High	Yes	No	0
2l	267.28	4	2	4	81.32	2.22	0.55	Moderate	High	No	No	0

[a] MW is the molecular weight, NHA is the number of hydrogen bond acceptors, NHD is the numbers of hydrogen bond donors, NRB is the number of rotatable bonds, TPSA is the topological polar surface area, *c*Log*P* is the logarithm of the octanol/water partition coefficient, *F* is the bioactivity score, GI is the gastrointestinal absorption, BBB is the blood–brain barrier permeation, Pgp is P-glycoprotein, and Ro5 is Lipinski's rule of five.

The in silico analysis showed that β-cyanoketones were not hepatotoxic, carcinogenic, immunotoxic, mutagenic, or cytotoxic (Table 2). The predicted LD_{50} values ranged from 180 to 3880 mg/kg, and the compounds were classified into six GHS (Globally Harmonized System of Classification and Labeling of Chemicals, rev. 8) categories *I*–*VI*: *I*, $LD_{50} \leq 5$ mg/kg; *II*, $5 < LD_{50} \leq 50$ mg/kg; *III*, $50 < LD_{50} \leq 300$ mg/kg; *IV*, $300 < LD_{50} \leq 2000$ mg/kg; *V*, $2000 < LD_{50} \leq 5000$ mg/kg; and *VI*, $LD_{50} > 5000$ mg/kg. Thus, software classified the toxicity of β-cyanoketones as follows: **2d**–**2f**, **2h**, and **2j** into *V*; **2a**, **2b**, **2g**, **2i**, **2k**, and **2l** into *IV*; and only **2c** into *III*. These results agreed with the absence of toxicity in *A. salina*.

Dihydrofolate reductase (DHFR) is required to maintain tetrahydrofolate (THF) metabolic levels. THF is a cofactor involved in the biosynthesis of purines and thymidine that are essential metabolites in living organisms, including Gram-negative bacteria *E. coli*. Consequently, DHFR from *E. coli* was selected as an antimicrobial target, and the chalcones active against *E. coli* showed high affinity for DHFR [24]. Taking into account structural similarity of chalcones **1** and β-cyanoketones **2**, it was reasonable to presume that the β-cyanoketones active against *E. coli* should inhibit DHFR.

The most active β-cyanoketones against *E. coli* (**2a**, **2b**, and **2f**) were docked into the *E. coli* DHFR active site. Previously, the molecular geometries of compounds to be docked were fully optimized. The analysis showed that these β-cyanoketones fit well in the binding cavity of DHFR; the binding energies ranged from –8.3 to –8.0 kcal/mol (Table 3) due to a number of hydrogen bonds and hydrophobic interactions (Fig. 1). β-Cyanoketone **2b** showed the highest in vitro activity against *E. coli*, whereas the docking results revealed hydrogen bonds between the cyano group at the β position and Ala13 residue at a distance of 2.58 Å and between the carbonyl group and Tyr108 at a distance of 3.07 Å (Figs. 1c, 1d). In addition, compound **2b** showed hydrophobic interactions between the methyl substituents and Ile26, Ile30, Ile56, Ala13, and Trp28. These interactions could stabilize the **2b**–DHFR complex and explain the antimicrobial activity of **2b** [41]. Compounds **2a** and **2b** showed similar binding energies (–8.3 kcal/mol) and interactions with DHFR (Table 3; Figs. 1a, 1b), but cyanoketone **2b** was involved in an additional hydrophobic interaction with Ile56 via methyl substituent (R^1). This may be responsible for the decreased antibacterial activity of **2a**. β-Cyanoketone **2f** formed an H bond between the cyano group and Ala13 with a bond distance of 2.45 Å.

Table 3. Docking interactions of β-cyanoketones **2a**, **2b**, and **2f** in the active site of *E. coli* dihydrofolate reductase (DHFR)

Compound no.	Score	Interaction	Interacting unit of the ligand	Amino acid	Distance, Å
2a	–8.3	H-Bond	CN	Ala13	2.50
		H-Bond	C=O	Tyr108	3.00
		Hydrophobic	Phenyl ring	Ala13	3.65
		Hydrophobic	CH_3	Ile26	3.52
		Hydrophobic	CH_3	Ile26	3.47
		Hydrophobic	CH_3	Trp28	3.61
		Hydrophobic	CH_3	Trp28	3.49
		Hydrophobic	CH_3	Ile30	3.53
		π-Stacking	Phenyl ring	Phe37	3.92
2b	–8.3	H-Bond	CN	Ala13	2.58
		H-Bond	C=O	Tyr108	3.07
		Hydrophobic	Phenyl ring	Ala13	3.63
		Hydrophobic	CH_3	Ile26	3.53
		Hydrophobic	CH_3	Ile26	3.45
		Hydrophobic	CH_3	Trp28	3.55
		Hydrophobic	CH_3	Trp28	3.51
		Hydrophobic	CH_3	Ile30	3.51
		Hydrophobic	CH_3	Ile56	3.75
		π-Stacking	Phenyl ring	Phe37	3.83
2f	–8.0	H-Bond	CN	Ala13	2.45
		Hydrophobic	Phenyl ring	Ala13	3.72
		Hydrophobic	CH_3	Ile26	3.52
		Hydrophobic	CH_3	Ile26	3.53
		Hydrophobic	CH_3	Trp28	3.65
		Hydrophobic	CH_3	Trp28	3.43
		Hydrophobic	CH_3	Ile30	3.58
		Hydrophobic	OCH_3	Phe37	3.95
		π-Stacking	Phenyl ring	Phe37	3.87

However, unlike **2a** and **2b**, **2f** did not form hydrogen bond between the carbonyl group and Tyr108 (Table 3; Figs. 1e, 1f); this could be due to the hydrophobic interaction between the methoxy group of **2f** and Phe37 residue, which explains its decreased antibacterial activity. These findings suggest that the antibacterial action of β-cyanoketones **2a**, **2b**, and **2f** is determined by the formation of adducts with DHFR involving the cyano and carbonyl groups of the ligand.

EXPERIMENTAL

The highest quality available reagents were purchased from Sigma–Aldrich (USA) and used without further purification. The reactions were performed in a CEM Discover SP Model 909150 single-mode microwave reactor equipped with an Explorer 12 Hybrid autosampler model 909505 (maximum power 725 W) at an initial power of 100 W using Pyrex tubes sealed

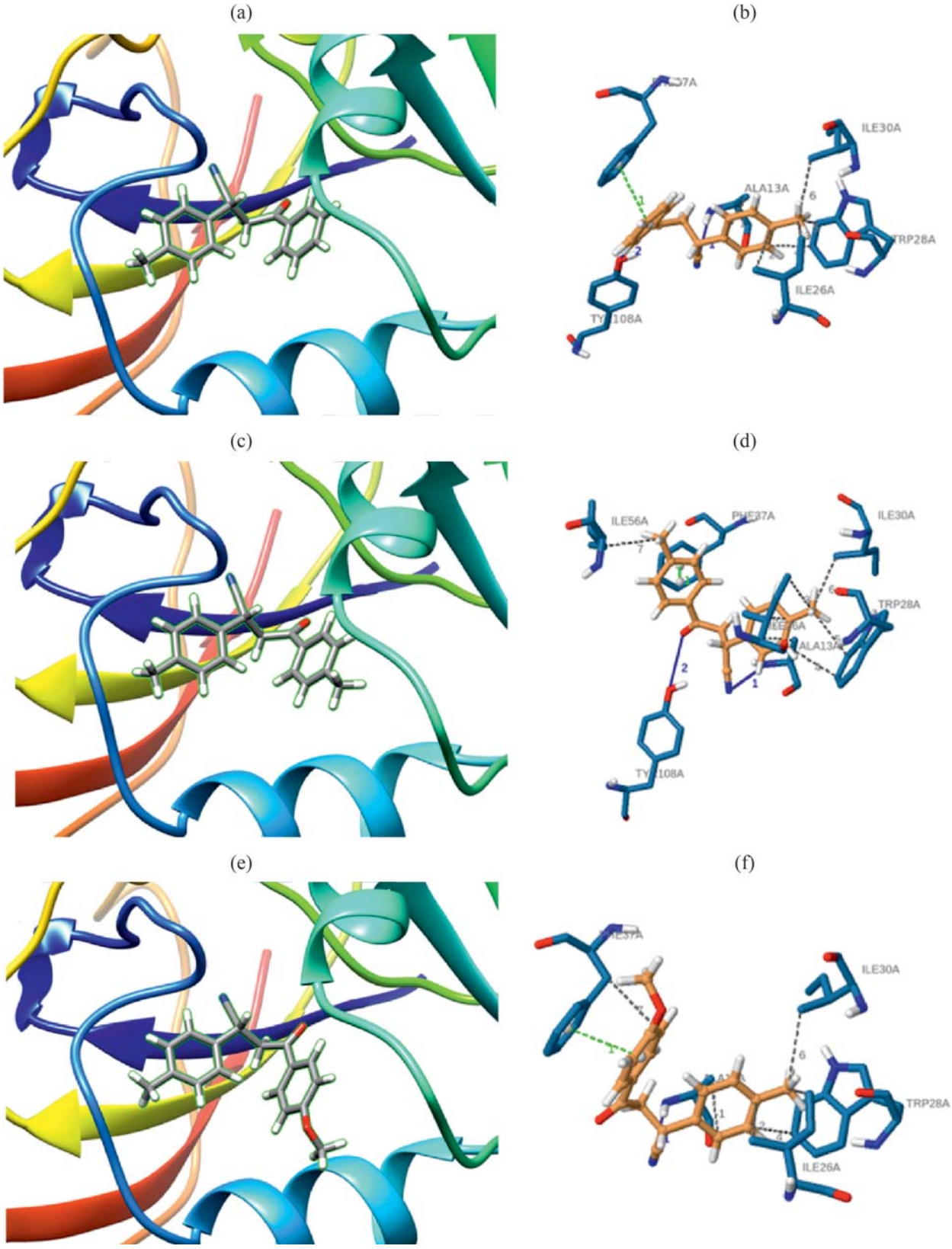

Fig. 1. 3D and 2D representations of the docking interactions of β-cyanoketones (a, b) **2a**, (c, d) **2b**, and (e, f) **2f** in the active site of *E. coli* DHFR.

with a silicone septum. The reactions were monitored by TLC on aluminum silica gel GF_{254} plates (0.25 mm) using different solvents as eluents. Chromatographic purifications were carried out in flash columns packed with silica gel 60 (230–400 mesh); elution was done with hexane–ethyl acetate mixtures. The melting points were determined using a Stuart SMP30 melting point apparatus; the reported values were averages of three separate measurements and are uncorrected. The Fourier transform IR spectra were recorded on a Cary 660 series FTIR-ATR spectrometer. The ^{1}H and ^{13}C NMR spectra were recorded on a JEOL Eclipse 400 spectrometer at 400 and 100 MHz, respectively, using $CDCl_3$ as solvent (unless otherwise stated) and internal standard. The chemical ionization mass spectra were obtained with a Varian Titan 4000 ion trap GC/MS instrument. Elemental analyses (C, H, N) of previously unknown compounds were performed on a Nova NanoSEM 200 coupled with an Oxford INCA X-Sight microanalysis system.

Synthesis of β-cyanoketones 2a–2l via the Bucherer–Bergs reaction under microwave irradiation (*general procedure*). A 10-mL pressure-rated vial was charged with chalcone **1a**–**1l** (1.0 mmol), potassium cyanide (4.0 mmol), ammonium carbonate (4.0 mmol), methanol (0.1 mL), and water (0.1 mL). The mixture was heated at 100°C for 20 min in a microwave reactor, cooled, and extracted with ethyl acetate. The product was purified by column chromatography using hexane–ethyl acetate (8:2) as eluent, followed by recrystallization from ethanol.

2-(4-Methylphenyl)-4-oxo-4-phenylbutanenitrile (2a). Yield 205 mg (83%), white solid, mp 132–134°C [14–17]. IR spectrum, ν, cm^{-1}: 2239, 1674. ^{1}H NMR spectrum, δ, ppm: 7.95–7.89 m (2H, H_{arom}), 7.63–7.55 m (1H, H_{arom}), 7.51–7.41 m (2H, H_{arom}), 7.31 d (J = 8.00 Hz, 2H, H_{arom}) 7.19 d (J = 6.0 Hz, 2H, H_{arom}), 4.53 d.d (J = 6.0, 6.0 Hz, 1H, CH), 3.71 d.d (J = 8.0, 18.0 Hz, 1H, CH_2), 3.48 d.d (J = 6.0, 18.0 Hz, 1H, CH_2), 2.34 s (3H, CH_3). ^{13}C NMR, δ_C, ppm: 194.7, 138.2, 135.6, 133.8, 132.2, 129.9, 128.9, 127.3, 120.8, 44.5, 32.6, 21.1. Mass spectrum (CI): m/z 250 $[M + H]^+$.

2,4-Bis(4-methylphenyl)-4-oxobutanenitrile (2b). Yield 213 mg (81%), white solid, mp 108–109°C [14]. IR spectrum, ν, cm^{-1}: 2241, 1668. ^{1}H NMR spectrum, δ, ppm: 7.82 d (J = 8.0 Hz, 2H, H_{arom}), 7.34–7.27 m (3H, H_{arom}), 7.23–7.16 m (3H, H_{arom}), 4.52 d.d (J = 8.0, 8.0 Hz, 1H, CH), 3.68 d.d (J = 8.0, 18.0 Hz, 1H, CH_2), 3.45 d.d (J = 6.0, 18.0 Hz, 1H, CH_2), 2.40 s (3H, CH_3), 2.34 s (3H, CH_3). ^{13}C NMR spectrum, δ_C, ppm: 194.2, 144.8, 138.1, 133.2, 132.2, 129.4, 128.3, 127.3, 120.9, 44.4, 31.6, 21.6. Mass spectrum (CI): m/z 263 $[M + H]^+$.

4-(4-Chlorophenyl)-4-oxo-2-(2,4,6-trimethylphenyl)butanenitrile (2c). Yield 187 mg (80%), yellowish white solid, mp 115–117°C. IR spectrum, ν, cm^{-1}: 2238, 1681. ^{1}H NMR spectrum, δ, ppm: 7.87 d (J = 8.0 Hz, 2H, H_{arom}), 7.45 d (J = 8.0 Hz, 2H, H_{arom}), 6.89 s (2H, H_{arom}), 5.00 d.d (J = 4.0, 6.0 Hz, 1H, CH), 3.88 d.d (J = 8.0, 18.0 Hz, 1H, CH_2), 3.23 d.d (J = 6.0, 18.0 Hz, 1H, CH_2), 2.48 s (6H, CH_3), 2.26 s (3H, CH_3). ^{13}C NMR spectrum, δ_C, ppm: 193.8, 140.4, 138.1, 136.2, 133.9, 130.3, 129.2, 128.4, 120.2, 40.9, 25.2, 20.7. Mass spectrum (CI): m/z 311 $[M + H]^+$. Found, %: C 73.49; H 6.19; N 4.02. $C_{19}H_{18}ClNO$. Calculated, %: C 73.19; H 5.82; N 4.49.

4-(4-Methoxyphenyl)-4-oxo-2-phenylbutanenitrile (2d). Yield 233 mg (88%), white solid, mp 103–105°C [14–17]. IR spectrum, ν, cm^{-1}: 2242, 1673. ^{1}H NMR spectrum, δ, ppm: 7.90 d (J = 10.0 Hz, 2H, H_{arom}), 7.47–7.32 m (5H, H_{arom}), 6.93 d (J = 8.0 Hz, 2H, H_{arom}), 4.57 d.d (J = 6.0, 8.0 Hz, 1H, CH), 3.87 s (3H, OCH_3), 3.68 d.d (J = 8.0, 18.0 Hz, 1H, CH_2), 3.44 d.d (J = 6.0, 18.0 Hz, 1H, CH_2). ^{13}C NMR spectrum, δ_C, ppm: 193.0, 164.0, 135.4, 130.5, 129.2, 128.7, 127.5, 120.7, 113.9, 55.5, 44.1, 31.9. Mass spectrum (CI): m/z 265 $[M + H]^+$.

2-(4-Methoxyphenyl)-4-oxo-4-phenylbutanenitrile (2e). Yield 244 mg (92%), white solid, mp 105–107°C [14–17]. IR spectrum, ν, cm^{-1}: 2237, 1676. ^{1}H NMR spectrum (DMSO-d_6), δ, ppm: 7.92 d (J = 6.0 Hz, 2H, H_{arom}), 7.59 m (J = 8.0 Hz, 1H, H_{arom}), 7.46 m (J = 8.0 Hz, 2H, H_{arom}), 7.34 d (J = 8.0, 2H, H_{arom}), 6.90 d (J = 8.0 Hz, 2H, H_{arom}), 4.52 d.d (J = 8.0, 8.0 Hz, 1H, CH), 3.80 s (3H, OCH_3), 3.68 d.d (J = 12.0, 20.0 Hz, 1H, CH_2), 3.48 d.d (J = 12.0, 20.0 Hz, 1H, CH_2). ^{13}C NMR spectrum (DMSO-d_6), δ_C, ppm: 194.8, 159.5, 135.7, 133.8, 128.8, 128.7, 128.1, 127.1, 120.8, 114.5, 55.3, 44.4, 31.2. Mass spectrum (CI): m/z 265 $[M + H]^+$.

4-(4-Methoxyphenyl)-2-(4-methylphenyl)-4-oxobutanenitrile (2f). Yield 232 mg (83%), white solid, mp 86–88°C [14]. IR spectrum, ν, cm^{-1}: 2246, 1666. ^{1}H NMR spectrum, δ, ppm: 7.90 d (J = 8.0 Hz, 2H, H_{arom}), 7.33–7.16 m (4H, H_{arom}), 6.93 d (J = 8.0, 2H, H_{arom}), 4.53 d.d (J = 6.0, 6.0 Hz, 1H, CH), 3.86 s (3H, OCH_3), 3.66 d.d (J = 8.0, 18.0 Hz, 1H, CH_2), 3.42 d.d (J = 6.0, 18.0 Hz, 1H, CH_2), 2.34 s (3H, CH_3). ^{13}C NMR spectrum, δ_C, ppm: 193.2, 163.9, 138.1, 132.3, 130.4, 129.8, 128.6, 127.2, 120.9, 113.8, 55.5,

44.1, 31.6, 20.9 ppm. Mass spectrum (CI): *m*/*z* 279 $[M + H]^+$.

2-(4-Methoxyphenyl)-4-(4-methylphenyl)-4-oxobutanenitrile (2g). Yield 253 mg (91%), white solid, mp 85–87°C [13]. IR spectrum, ν, cm^{-1}: 2250, 1669. ^1H NMR spectrum, δ, ppm: 7.87 d (*J* = 8.0 Hz, 2H, H_{arom}), 7.38 d (*J* = 8.0 Hz, 2H, H_{arom}), 7.30 d (*J* = 8.0, 2H, H_{arom}), 6.92 d (*J* = 8.0, 2H, H_{arom}), 4.51 d.d (*J* = 8.0, 8.0 Hz, 1H, CH), 3.78 s (3H, OCH_3), 3.74 d.d (*J* = 8.0, 18.0 Hz, 1H, CH_2), 3.56 d.d (*J* = 8.0, 18.0 Hz, 1H, CH_2), 2.39 s (3H, CH_3). ^{13}C NMR spectrum, δ_C, ppm: 195.5, 159.6, 144.6, 133.6, 129.0, 128.4, 127.9, 127.5, 121.0, 114.1, 54.4, 43.5, 30.9, 20.2. Mass spectrum (CI): *m*/*z* 279 $[M + H]^+$.

2,4-Bis(4-methoxyphenyl)-4-oxobutanenitrile (2h). Yield 168 mg (87%), yellowish orange solid, mp 100–102°C. IR spectrum, ν, cm^{-1}: 2244, 1672. ^1H NMR spectrum, δ, ppm: 7.90 d (*J* = 8.0, 2H, H_{arom}), 7.34 d (*J* = 8.0, 2H, H_{arom}), 6.96–6.86 m (4H H_{arom}), 4.52 d.d (*J* = 6.0, 8.0 Hz, 1H, CH), 3.86 s (3H, OCH_3), 3.80 s (3H, OCH_3) 3.64 d.d (*J* = 6.0, 18.0 Hz, 1H, CH_2), 3.42 d.d (*J* = 8.0, 18.0 Hz, 1H, CH_2). ^{13}C NMR spectrum, δ_C, ppm: 193.1, 163.9, 130.5, 130.2, 128.8, 127.3, 121.0, 114.4, 113.8, 55.6, 44.1, 31.1. Mass spectrum (CI): *m*/*z* 295 $[M + H]^+$. Found, %: C 73.15; H 5.96; N 4.14. $C_{18}H_{17}NO_3$. Calculated, %: C 73.20; H 5.80; N 4.74.

2-(4-Chlorophenyl)-4-(4-methoxyphenyl)-4-oxobutanenitrile (2i). Yield 150 mg (80%), white solid, mp 88–90°C. IR spectrum, ν, cm^{-1}: 2243, 1670. ^1H NMR spectrum, δ, ppm: 7.90 d (*J* = 10.0 Hz, 2H, H_{arom}), 7.36 s (3H, H_{arom}), 6.93 d (*J* = 8.0 Hz, 2H, H_{arom}), 4.56 d.d (*J* = 6.0, 8.0 Hz, 1H, CH), 3.87 s (3H, OCH_3), 3.67 d.d (*J* = 8.0, 18.0 Hz, 1H, CH_2), 3.44 d.d (*J* = 8.0, 18.0 Hz, 1H, CH_2). ^{13}C NMR spectrum, δ_C, ppm: 192.9, 164.1, 134.3, 133.8, 130.5, 130.3, 128.9, 128.5, 120.4, 113.9, 55.6, 43.8, 31.4. Mass spectrum (CI): *m*/*z* 300 $[M + H]^+$. Found, %: C 68.18; H 5.08; N 4.41. $C_{17}H_{14}ClNO_2$. Calculated, %: C 68.12; H 4.71; N 4.67.

4-Oxo-4-phenyl-2-{4-[(4*H*-pyran-3-yl)oxy]-phenyl}butanenitrile (2j). Yield 304 mg (50%), light green solid, mp 96–99°C. IR spectrum, ν, cm^{-1}: 2237, 1676. ^1H NMR spectrum, δ, ppm: 7.92 d (*J* = 6.0 Hz, 2H, H_{arom}), 7.47 m (5H, H_{arom}), 7.07 d (*J* = 8.0 Hz, 2H, H_{arom}), 5.41 s (1H, pyran), 4.52 d.d (*J* = 6.0, 8.0 Hz, 1H, CH), 3.7 d.d (*J* = 6.0, 18.0 Hz, 1H, CH_2), 3.48 d.d (*J* = 6.0, 18.0, 1H, CH_2), 1.72–1.50 m (6H, pyran). ^{13}C NMR spectrum, δ_C, ppm: 194.7, 156.7, 148.4, 146.1, 135.7, 133.9, 128.8, 127.9, 116.95, 96.5, 61.9, 44.6, 31.2, 30.2, 24.9, 18.6 ppm. Mass spectrum (CI): *m*/*z* 331 $[M + H]^+$. Found, %: C 74.60; H 5.51; N 3.67. $C_{21}H_{17}NO_3$. Calculated, %: C 73.12; H 5.30; N 3.88.

2-(4-Hydroxyphenyl)-4-oxo-4-phenylbutanenitrile (2k). Yield 106 mg (72%), bluish green solid, mp 146–149°C. IR spectrum, ν, cm^{-1}: 2240, 1674. ^1H NMR spectrum (DMSO-d_6), δ, ppm: 7.93 d (*J* = 4.0 Hz, 2H, H_{arom}), 7.66 t (*J* = 8.0 Hz, 1H, H_{arom}), 7.46 m (3H, H_{arom}), 7.23 d (*J* = 8.0 Hz, 2H, H_{arom}), 6.85 d (*J* = 8.0 Hz, 2H, H_{arom}), 4.45 d.d (*J* = 4.0, 8.0 Hz, 1H, CH), 3.69 d.d (*J* = 12.0, 20.0 Hz, 1H, CH_2), 3.47 d.d (*J* = 12.0, 20.0 Hz, 1H, CH_2). ^{13}C NMR spectrum (DMSO-d_6), δ_C, ppm: 195.1, 157.4, 135.6, 133.6, 1284, 127.9, 125.3, 121.1, 115.9, 44.4, 40.2, 31.2. Mass spectrum (CI): *m*/*z* 251 $[M + H]^+$. Found, %: C 72.75; H 5.41; N 6.88. $C_{16}H_{13}NO_2$. Calculated, %: C 76.48; H 5.21; N 5.57.

2-(3,4-Dihydroxyphenyl)-4-oxo-4-phenylbutanenitrile (2l). Yield 118 mg (74%), reddish brown solid, mp 105–108°C. IR spectrum, ν, cm^{-1}: 2240, 1676. ^1H NMR spectrum, δ, ppm: 8.47 s (2H, OH), 7.94 d (*J* = 10.0 Hz, 2H, H_{arom}), 7.43 m (4H, H_{arom}), 6.72 m (3H, H_{arom}), 4.26 d.d (*J* = 4.00, 6.00 Hz, 1H, CH), 3.60 d.d (*J* = 6.0, 18.0 Hz, 1H, CH_2), 3.37 d.d (*J* = 4.0, 20.0 Hz, 1H, CH_2). ^{13}C NMR spectrum, δ_C, ppm: 195.4, 145.2, 135.7, 133.8, 128.9, 128.0, 126.3, 121.1, 118.5, 44.5, 40.2, 31.0. Mass spectrum (CI): *m*/*z* 267 $[M + H]^+$. Found, %: C 76.84; H 5.29; N 5.77. $C_{16}H_{13}NO_3$. Calculated, %: C 71.90; H 4.90; N 5.24.

Antibacterial activity. Seven human pathogenic bacteria were used for the antibacterial assay: four ATCC (*Staphylococcus aureus* 29213, *Enterococcus faecalis* 29212, *Pseudomonas aeruginosa* 27853, and *Escherichia coli* 25922) (DIFCO Laboratory, Michigan, USA) and three clinical isolates (*Salmonella* group D, *Shigella dysenteriae*, and *Escherichia coli*) provided by the Laboratory of Bacteriology of the National Institute of Pediatrics, Mexico City, Mexico.

The minimum inhibitory concentrations (MIC) were determined by microdilution assay using 96-well plates according to the National Committee for Clinical Laboratory Standards recommendations [27]. The bacterial strains were cultured in Petri dishes with Muller–Hinton agar at 37°C for 18–24 h; the colonies were suspended in 1 mL of 0.85% NaCl (w/v), and the density was adjusted to 10^8 CFU/mL (0.5 McFarland turbidity). The bacterial suspension was diluted to 10^6 CFU/mL; 50 μL was inoculated per well, and 50 μL of a β-cyanoketone solution at each concentration was added. The positive control was Gentamicin

(0.5–4 μg/mL), the negative growth control was bacterial culture without additives, and the negative toxicity control was bacterial culture with the solvent used to dissolve the compounds. The 96-well microplates were incubated at 37°C for 18–24 h. After incubation, the MIC value corresponded to the lowest concentration at which no turbidity or button formation was observed. The minimum bactericidal concentration (MBC) was determined based on the results of the MIC assay. Tryptic soy agar (TSA) plates were inoculated with aliquots of every well of the MIC assay where bacterial growth was not observed, including that with the MIC value, and incubated at 37°C for 18–20 h. The MBC value corresponded to that of the well with the minimal extract concentration that prevented bacterial growth in the TSA plates. All assays were carried out in triplicate.

Acute toxicity assay (*Artemia salina*). The acute toxicity was determined by inhibiting the mobility of the crustacean *A. salina*, after 24 and 48 h of exposure, according to the procedure established by the OECD (Organization for Economic Cooperation and Development) [28]. The *A. salina* eggs were hatched in artificial seawater prepared with 38 g/L of sea salt (Instant Ocean®, Blacksburg, VA, USA) and oxygenated with an aquarium pump. The temperature was kept in an optimal range of 25–30°C and under a light source (white neon, 70 W) for 48 h. The compounds were dissolved in DMSO (5%, 20 mg/mL), and four dilutions were prepared (1000, 500, 100, and 10 ppm). The toxicity assay was carried out in 4-mL test tubes, and each concentration was evaluated in triplicate. First, ten nauplii were added to each tube in a volume not exceeding 0.5 mL using a Pasteur pipette, 100 μL of a compound dilution (1000, 500, 100, and 10 ppm) was added, and the final volume was adjusted to 2 mL with seawater. The tubes were then incubated at 25°C for 24 h under artificial light. After the incubation, the dead and alive nauplii were counted; each tube was added with 50 μL of formaldehyde (10% v/v) and let stand for 15 min to kill the remaining alive nauplii. Finally, the total number of nauplii per tube was counted. The results were reported as mortality percentages, determined by the correction of the Abbott formula [29]:

$$\% \text{ Mortality} = (\text{DLT}/\text{ALT})\times 100,$$

where DLT is the number of dead Larvae in the tube, and ALT is the number of alive larvae in the tube.

In silico estimation of physicochemical and pharmacokinetic parameters. Physicochemical and pharmacokinetic parameters and drug-likeness of the synthesized β-cyanoketones were predicted using SwissADME (http://www.swissadme.ch/index.php). The 2D structures of β-cyanoketones were drawn using Marvin Sketch (ChemAxon, Version 18.30) and converted into SMILEY mode by online SMILES translator available in SwissADME [30, 31].

Toxicity prediction. The toxicity of the synthesized β-cyanoketones was predicted with the ProTox-II webserver [32, 33], registering the following toxicity endpoints: predicted median lethal dose (LD_{50}) in rodents; organ toxicity (hepatotoxicity); and toxicity endpoints including carcinogenicity, immunotoxicity, mutagenicity, and cytotoxicity.

Molecular docking studies. Initially, the predicted 3D structure of the DHFR was established with the online tools Phyre 2 and Swiss-Model and visualized with Chimera [34]. The 3D model structure was refined using the GalaxyWEB server [35], and its quality and reliability were confirmed with different online tools. The stereochemical aspects of *E. coli* DHFR were inspected through a Ramachandran plot, in which 91.0% of the residues were in the most favored region. Moreover, the *Z* score calculated with ProSA was –6.02, indicating a good quality of the DHFR model. The model was also validated with the PROCHECK online server, giving 98.88 and 97.06 overall quality factors in ERRAT and 97.32% score in VERIFY 3D [36]. The three-dimensional structures of β-cyanoketones were generated through their SMILES string using UCSF Chimera [34]. Energy minimization of the models was done employing Chimera's default conditions with MMTK and Antechamber parameters. Then, the docking between the most active β-cyanoketones **2a**, **2b**, and **2f** and *E. coli* DHFR was performed using the Achilles Blind Docking Web Server (https://bio-hpc.ucam.edu/aquiles). Fifty docking poses were generated for each ligand and sorted according to the binding energy and conformation in the protein active site. All docked images were visualized using UCSF Chimera [34] and analyzed through protein–ligand identifier profiler (PLIP) BIOTEC TU Dresden.

CONCLUSIONS

The Bucherer-Bergs reaction was applied as a novel and attractive method for the direct hydrocyanation of α,β-unsaturated ketones to synthesize β-cyanoketones from chalcones using KCN and $(NH_4)_2CO_3$ in $MeOH/H_2O$ under microwave irradiation without the formation of HCN. The reaction was fast and regio-

selective, and it provided moderate to high yields; in addition, the employed reagents were readily available and easily handled. β-Cyanoketones **2a**, **2b**, **2d**–**2i**, **2k**, and **2l** with antibacterial activity were nontoxic in the *Artemia salina* model. Five of them (**2a**, **2b**, **2f**, **2g**, and **2i**) exhibited moderate antimicrobial activities against *E. coli* (ATCC 25922), the most active being those with an activating group (e.g., Me) in R^4 (**2a**, **2b**, and **2f**) and especially **2b** ($R^1 = R^4 = Me$). The substitution pattern in the antibacterial β-cyanoketones could decrease the molecular polarity and hence the movement through *E. coli* membrane. In silico analysis of **2a**, **2b**, and **2f** suggested their good pharmacokinetics, drug-likeness, and toxicity properties, and they could be safely used. Moreover, the docking with DHFR showed that the cyano and carbonyl groups in β-cyanoketones were essential for their antibacterial activity. The results suggested that the synthesized β-cyanoketones could be used to develop new chemical structures with improved or novel biological activities.

ACKNOWLEDGMENTS

M.A. Leyva Acuña is grateful to Consejo Nacional de Ciencia y Tecnología (CONACYT) for the graduate studies scholarship. We would like to thank Dr. V.C. Osuna Galindo, Centro de Investigación en Materiales Avanzados, S.C. (Chihuahua, Mexico) for the elemental analyses.

FUNDING

This project was partially funded by the National Council of Science and Technology of Mexico (CONACYT) under Grant no. A1-S-24537 and "Programa de Fomento y Apoyo a Proyectos de Investigación" (PROFAPI) of the Autonomous University of Sinaloa under Grant no. PROFAPI2015/185.

CONFLICT OF INTEREST

The authors declare no conflict of interest.

REFERENCES

1. Church, N.A. and McKillip, J.L., *Biologia*, 2021, vol. 76, p.1535. https://doi.org/10.1007/s11756-021-00697-x
2. Egelkamp, R., Zimmermann, T., Schneider, D., Hertel, R., and Daniel, R., *Front. Environ. Sci*., 2019, vol. 7, p. 103. https://doi.org/10.3389/fenvs.2019.00103
3. Wang, X., Wang, Y., Li, X., Yu, Z., Song, C., and Du, Y., *RSC Med. Chem*., 2021, vol. 12, p. 1650. https://doi.org/10.1039/D1MD00131K
4. Tanaka, Y., Kanai, M., and Shibasaki, M., *J. Am. Chem. Soc*., 2008, vol. 2, p. 9911. https://doi.org/10.1021/ja801201r
5. Nandi, S., Patel, P., Jakhar, A., Khan, N.H., Biradar, A.V., and Kureshy, R.I., *ChemistrySelect*, 2017, vol. 2, p. 9911. https://doi.org/10.1002/slct.201702196
6. Hu, Z., Dong, J., Li, Z., Yuan, B., Wei, R., and Xu, X., *Org. Lett*., 2018, vol. 20, p. 6750. https://doi.org/10.1021/acs.orglett.8b02870
7. Jiang, D., Wang, Y.Y., Tu, M., and Dai, L.Y., *React. Kinet. Catal. Lett*., 2008, vol. 95, p. 265. https://doi.org/10.1007/s11144-008-5345-8
8. Wu, L., Wang, L., Chen, P., Guo, Y.L., and Liu, G.J., *Adv. Synth. Catal*., 2020, vol. 362, p. 2189. https://doi.org/10.1002/adsc.202000202
9. Winkler, C.K., Clay, D., Turrini, N.G., Lechner, H., Kroutil, W., and Davies, S., *Adv. Synth. Catal*., 2014, vol. 356, p. 1878. https://doi.org/10.1002/adsc.201301055
10. Sammis, G.M. and Jacobsen, E.N., *J. Am. Chem. Soc*., 2003, vol. 125, p. 4442. https://doi.org/10.1021/ja034635k
11. Mita, T., Sasaki, K., Kanai, M., and Shibasaki, M., *J. Am. Chem. Soc*., 2005, vol. 127, p. 514. https://doi.org/10.1021/ja043424s
12. Ramesh, S. and Lalitha, A., *Acta. Chim. Slov*., 2013, vol. 60, p. 689.
13. Dong, H.R., Dong, W.J., Li, R.S., Hu, Y.M., Dong, H.S., and Xie, Z.X., *Green Chem*., 2014, vol. 16, p. 3454. https://doi.org/10.1039/C4GC00386A
14. Li, Z. and Yin, J., *Chin. J. Chem*., 2017, vol. 35, p. 1179. https://doi.org/10.1002/cjoc.201600860
15. Li, Z.F., Li, Q., Ren, L.Q., Li, Q.H., Peng, Y.G., and Liu, T.L., *Chem. Sci*., 2019, vol. 10, p. 5787. https://doi.org/10.1039/C9SC00640K
16. Ni, J., Cristòfol, À., and Kleij, A.W., *Org. Chem. Front*., 2021, vol. 8, p. 4520. https://doi.org/10.1039/D1QO00770J
17. Iida, H., Moromizato, T., Hamana, H., and Matsumoto, K., *Tetrahedron Lett*., 2007, vol. 48, p. 2037. https://doi.org/10.1016/j.tetlet.2006.12.145
18. Yang, J. and Chen, F., *Chin. J. Chem*., 2010, vol. 28, p. 981. https://doi.org/10.1002/cjoc.201090182
19. Strappaveccia, G., Angelini, T., Bianchi, L., Santoro, S., Piermatti, O., and Lanari, D., *Adv. Synth. Catal*., 2016, vol. 13, p. 2134. https://doi.org/10.1002/adsc.201600287
20. Fleming, F.F., Yao, L., Ravikumar, P., Funk, L., and Shook, B.C., *J. Med. Chem*., 2010, vol. 53, p. 7902. https://doi.org/10.1021/jm100762r
21. Montes-Avila, J., Díaz-Camacho, S.P., Sicairos-Félix, J., Delgado-Vargas, F., and Rivero, I.A., *Bioorg. Med. Chem*., 2009, vol. 17, p. 6780. https://doi.org/10.1016/j.bmc.2009.02.052

22. Díaz-Carrillo, J.T., Díaz-Camacho, S.P., Delgado-Vargas, F., Rivero, I.A., López-Angulo, G., Sarmiento-Sánchez, J.I., and Montes-Avila, J., *Braz. J. Pharm. Sci*., 2018, vol. 54, article ID e17343. https://doi.org/10.1590/s21759790201800031734 3
23. Srinivasan, B., Rodrigues, J.V., Tonddast-Navaei, S., Shakhnovich, E., and Skolnick, J., *ACS Chem. Biol*., 2017, vol. 12, p. 1848. https://doi.org/10.1021/acschembio.7b00175
24. Benmekhbi, L., Krid, A., Bencharif, L., and Bencharif, M., *Int. J. Appl. Phys. Bio-Chem. Res*., 2014, vol. 4, p. 17.
25. Alrohily, W.D., Habib, M.E., El-Messery, S.M., Alqurshi, A., El-Subbagh, H., and Habib, E.S., *Microb. Pathog*., 2019, vol. 136, p. 103674. https://doi.org/10.1016/j.micpath.2019.103674
26. Wróbel, A., Maliszewski, D., Baradyn, M., and Drozdowska, D., *Molecules*, 2019, vol. 25, article no. 116. https://doi.org/10.3390/molecules25010116
27. Weinstein, M.P., National Committee for Clinical Laboratory Standards, Wayne: New Jersey, 2018.
28. Nunes, B.S., Carvalho, F.D., Guilhermino, L.M., and Van-Stappen, G., *Environ. Pollut*., 2006, vol. 144, p. 453. https://doi.org/10.1016/j.envpol.2005.12.037
29. Abbott, W.S., *J. Econ. Entomol*.,1925, vol. 18, p. 265. https://doi.org/10.1093/jee/18.2.265a
30. Kaur, G., Kaur, M., Sharad, L., and Bansal, M., *J. Heterocycl. Chem*., 2020, vol. 57, p. 225. https://doi.org/10.1002/jhet.3768
31. Erol, M., Celik, I., Temiz-Arpaci, O., Goker, H., Kaynak-Onurdag, F., and Okten, S., *Med. Chem. Res*., 2020, vol. 29, p. 2028. https://doi.org/10.1007/s00044-020-02621-5
32. Banerjee, P., Eckert, A.O., Schrey, A.K., and Preissner, R., *Nucleic Acids Res*., 2018, vol. 46, p. W257. https://doi.org/10.1093/nar/gky318
33. Egbujor, M.C., Okoro, U.C., and Okafor, S., *Med. Chem. Res*., 2019, vol. 28, p. 2118. https://doi.org/10.1007/s00044-019-02440-3
34. Pettersen, E.F., Goddard, T.D., Huang, C.C., Couch, G.S., Greenblatt, D.M., and Meng, E.C., *J. Comput. Chem*., 2004, vol. 25, p. 1605. https://doi.org/10.1002/jcc.20084
35. Ko, J., Park, H., Heo, L., and Seok, C., *Nucleic Acids Res*., 2012, vol. 40, p. W294. https://doi.org/10.1093/nar/gks493
36. Lomize, M.A., Pogozheva, I.D., Joo, H., Mosberg, H.I., and Lomize, A.L., *Nucleic Acids Res*., 2014, vol. 40, p. D370. https://doi.org/10.1093/nar/gkr703
37. Rivero, I.A., Reynoso-Soto, E.A., and Ochoa-Terán, A., *Arkivoc*, 2011, vol. 2011, part (ii), p. 260. https://doi.org/10.3998/ark.5550190.0012.221
38. Kalník, M., Gabko, P., Bella, M., and Koóš, M., *Molecules*, 2021, vol. 26, article no. 4024. https://doi.org/10.3390/molecules26134024
39. Li, Z., Liu, C., Zhang, Y., Li, R., Ma, B., and Yang, J., *Synlett*, 2012, vol. 23, p. 2567. https://doi.org/10.1055/s-0032-1317179
40. Bhat, A.R., Dongre, R.S., Almalki, F.A., Berredjem, M., Aissaoui, M., and Touzani, R., *Bioorg. Chem*., 2021, vol. 106, article ID 104480. https://doi.org/10.1016/j.bioorg.2020.104480
41. Dongre, R.S., Meshram, J.S., Selokar, R.S., Almalki, F.A., and Hadda, T.B., *New. J. Chem*., 2018, vol. 42, p. 15610. https://doi.org/10.1039/C8NJ02081G
42. de Jesús Uribe-Beltrán, M., Ahumada-Santos, Y.P., Díaz-Camacho, S.P., Eslava-Campos, C.A., Reyes-Valenzuela, J.E., and Báez-Flores, M.E., *J. Med. Microbiol*., 2017, vol. 66, p. 972. https://doi.org/10.1099/jmm.0.000548
43. Lipinski, C.A., *Adv. Drug Delivery Rev*., 2016, vol. 101, p. 34. https://doi.org/10.1016/j.addr.2016.04.029